Evaluation of hardness, wear rate, and thermal stability of epoxy composites reinforced with synthesized *Mangifera indica* shell ash and cow bone ash hybrid particulates

Clement Nworji Obiora*, Callistus Nkemjika Chukwu, Ugochukwu Richards Orji, Sunday Chimezie Anyaora, Nwekeoti Arinze Chukwunakueze, Fakiyesi Oladapo Babafemi

Nnamdi Azikiwe University Awka, Anambra State, Nigeria
*Corresponding author, email: cn.obiora@unizik.edu.ng

Article history
Submitted: 20 July 2026
Revised: 25 August 2026
Accepted: 3 August 2026
Published: 7 September 2026

Keywords
Cow bone ash
Hybrid composites
Mangifera indica shell ash
Thermal stability
Wear resistance

Abstract
This study evaluated the hardness, sliding wear behavior, and thermal stability of epoxy-based hybrid composites reinforced with synthesized *Mangifera indica* shell ash (MISA) and cow bone ash (CBA). Surface modification parameters of the hybrid filler were optimized using Central Composite Design (CCD) within the Response Surface Methodology (RSM) framework to improve matrix compatibility and interfacial bonding. Hybrid composite specimens containing a fixed filler content were fabricated through the hand lay-up technique and characterized through mechanical, tribological, spectroscopic, and thermogravimetric analyses. Hardness testing revealed enhanced surface rigidity and matrix densification, indicating that the inorganic filler phases effectively filled micro voids and restricted localized deformation. Tribological evaluation under dry sliding conditions demonstrated low specific wear rates and improved wear resistance, attributed to reduced material loss and the formation of a protective transfer film at the contact interface. Fourier Transform Infrared (FTIR) spectroscopy confirmed the presence of hydroxyl, aliphatic, carbonyl, and aromatic functional groups, verifying the formation of a hybrid organic–inorganic composite structure. Thermogravimetric analysis (TGA) showed a multi-stage degradation pattern and increased residual char content, indicating that the ash network acted as an effective barrier against thermal decomposition and enhanced thermal stability. The results demonstrate that hybridization of plant- and animal-derived waste particulates provides a cost-effective and sustainable approach for improving the surface durability, wear resistance, and thermal performance of epoxy composites. These findings highlight the potential of MISA/CBA-reinforced epoxy composites for lightweight structural and engineering applications.

1. Introduction

The use of agro-waste or animal derived waste as hybrid reinforcement with polymer matrix is a significant step in the field of eco-friendly material science. The epoxy resin is used as a versatile thermosetting matrix material with good mechanical properties, chemical resistance and dimensional stability. The inherent properties of unreinforced epoxy are subject to a number of weaknesses, such as brittle failure modes, high surface friction under sliding conditions and thermal degradation at high temperatures. The synthesized *Mangifera indica* (mango shell) ash and cow bone ash hybrid particulates when reinforced in epoxy has an enhanced mechanical, tribological and thermal properties of the composite [1].

Hardness is one of the important parameters used to assess the resistance to surface deformation and density of a composite matrix. Indentation tests (Brinell and Leeb hardness) are used to assess the material's ability to resist loaded contact areas. When cow bone ash and mango seed shell ash are uniformly distributed in the epoxy resin, the overall hardness is increased. The inorganic calcium phosphate mineral, hydroxyapatite is in very high concentration in cow bone ash and gives the polymer great inherent rigidity. The mango seed shell ash is rich in hard silica, alumina, and carbonaceous phases which can effectively plug in the micro-voids in hand-lay-up processing [2]. In combination these particulates decrease the mobility of the polymer chains making plastic deformation under mechanical indentation more difficult. Sodium hydroxide treatment of the surface eliminates loose organic contaminants and makes the surface rougher, resulting in good mechanical interlocking between the particulate reinforcement and the epoxy binder. As the particulate loading is increased beyond an optimum level, localized shear deformation is limited which results in increased hardness of the material as compared to neat epoxy resin [3].

© 2026 The Author(s)
This work is licensed under a Creative Commons Attribution-ShareAlike 4.0 International License
ISSN: 3110-1577

The tribological performance, which was determined by a certain wear rate and wear resistance under dry sliding conditions, has a significant dependence on the dispersion of the fillers, applied load and adhesion between the surfaces. Unreinforced epoxy is often subjected to high adhesive and abrasive wear against metal counter faces which causes significant removal of material. Synthetic hybrid ash particulates alter the wear mode from micro-ploughing to micro-scratching [4]. When in dry sliding contact, the hard ceramic and mineral phases of mango seed shell ash and cow bone ash are acting as the load-bearing components, and protecting the polymer matrix from direct abrasive contact. In continuous sliding, the fine particulate debris will detach, leaving a stable film of debris on the counter face interface to reduce the friction coefficient and prevent high friction to cause severe wear. Surface treatment of the fillers is important and should be done properly to get good bonding between the surfaces during contact, that is, to avoid early pull-out. The tensile force of the interface is maintained, which helps to retain the hybrid particles in the epoxy matrix and provides low specific wear and good wear resistance under high normal loads [5].

Thermal stability is also an important performance criterion for the structural polymer composites especially in the applications where high temperature conditions are present. The neat epoxy is shown to be thermally unstable by the thermogravimetric analysis (TGA) and differential thermal analysis (DTA). The large mass loss between 300°C and 450°C occurs as the crosslinked polymer chains in the epoxy cleave thermally. The inclusion of synthesized *Mangifera indica* shell ash and cow bone ash makes the thermal degradation temperature of the structure be pushed to higher temperatures [6]. The inorganic mineral components of cow bone ash and refractoriness of silica and alumina in mango seed shell ash acts as good thermal barrier to slow heat transfer through the polymer bulk. These ash particulates are non-combustible, adding to the volatile organic matrix mass, and during heating, forming a protective char layer that prevents oxygen diffusion and at the same time traps volatile degradation products. With the hybrid particulate system, the overall yields of residual char at 900°C have been improved while the overall mass loss rates have been reduced, showing higher levels of thermal stability than unreinforced matrix formulations [7].

The synergies that occur between animal and agro-waste particulates in epoxy matrices emphasize the improvement in a combination of properties such as hardness, wear resistance and thermal behavior. Using Response Surface Methodology, the parameters of surface modification (sodium hydroxide concentration, treatment time) are optimized to ensure the best possible balance between the strength of the interfacial bond and structural integrity. The resulting hybrid composite material is a low cost, lightweight and sustainable solution for high demanding engineering applications such as automotive parts, structural panels and wear-resistant elements of machines. Unreinforced epoxy matrices are very brittle, have high wear rates under dry sliding contact and low thermal stability at high temperatures. Previous research has investigated individual natural fillers such as bone ash or plant fibers for enhancing polymer properties [8]; [9]. But there are some agro-wastes that are generally lacking in the proper proportions of hard and thermal resistant inorganic phases. Cow bone ash containing bio-calcite and *Mangifera indica* shell ash containing silica is a yet unexplored synergy. The hardness, wear rate and thermal stability of this particular hybrid particulate system will be investigated, which will fulfil the need for low cost and eco-friendly epoxy composites with demanding structural applications.

2. Method

2.1. Materials Sourcing and Equipment

High grade EPOCHEM 105 (clear epoxy resin) was purchased from GZ Industrial Supplies, Port Harcourt, Rivers State, Nigeria while EPOCHEM 205 (catalyst/hardener) was purchased from the same source. The mold release agent used was obtained from Enugu state of Nigeria, 2% of sulfuric acid was obtained from Enugu state, distilled water was obtained from the laboratory and laboratory filter paper was obtained from Enugu state, while sodium hydroxide ("NaOH") pellets (LR grade) were obtained from Molychem Industry, Mumbai, India. The raw materials for the reinforcement namely *Mangifera indica* (mango) seeds and cow bones were collected from the Metallurgical Training Institute (MTI) in Onitsha of the state of Anambra state and Amansea Abattoir, Awka in the same state respectively.

Laboratory instruments used during the processing and characterization phases were: 1) a BL20001 electronic compact balance, 2) a KW-1000DC digital water bath (HH-2), 3) glass molds, 4) a muffle furnace, 5) magnetic stirrers, 6) a lyophilizing machine (Model: Wincom FD-10S), 7) a digital motorized Brinell hardness tester (Model: Phase II 900-355), 8) an automated universal tensile testing machine (Model: JPL130812), 9) an RT-104 Pin-on-Disc wear tester, 10) an optical microscope (Model: L2003A), 11) a Scanning Electron Microscope (Model: LEO-430i) with an attached Energy Dispersive Spectroscopy system (Model: LINK-ISIS-300), 12) an infrared spectrophotometer (Model: M530), 13) a thermal analyzer (Model: TGA 4000) from PerkinElmer.

© 2026 The Author(s)
This work is licensed under a Creative Commons Attribution-ShareAlike 4.0 International License
ISSN: 3110-1577

2.2. Particulate Synthesis and Filler Preparation

Cow bones and *Mangifera indica* seeds were sourced and washed with distilled water and left to dry under the sun without any other chemical agents before the extraction of their seed shells in order to prevent contamination. The ground dried bones and dried mango shell were ball-milled to fine powder and classified using a 180 μm hand sieve. Equal mass proportions (1:1 ratio) of the 180 μm bone and mango shell powders were combined to yield the baseline bone/mango seed ash (B/M) hybrid filler.

To synthesize in hydrothermal method, the particulate mixture was carburized in a muffle furnace for 4 hours at 400°C. This ash was then stirred in distilled water for 4 hours at 150°C with a magnetic stirrer and the resulting ash was taken out. After filtration, the ash residue obtained was calcined at 400°C to get the final synthesized ash particulates. Figure 1 shown the bones and the *Mangifera indica* seeds.



Figure 1. The bones and the *Mangifera indica* seeds

2.3. Surface Modification and Design of Experiment

Response Surface Methodology (RSM) based on Central Composite Design (CCD) was used to optimize the surface treatment parameters, and the software MINITAB 16 and Design-Expert were used. The full-factorial CCD consisted of 13 complete experimental runs, plus five center points and four axial points, and two factors, each with two levels. The factors evaluated were concentration of NaOH (2-10%) and duration of treatment (1-5 hours). Alkaline surface modification was carried out by soaking portions of the 180 μm B/M hybrid powder in varying concentrations of NaOH solution at 60°C according to the RSM design matrix. Following treatment, the mixtures were filtered, neutralized with 2% H_2SO_4, and rinsed with distilled water to remove residual dissolved ions and surface impurities. The purified, treated particulates were then freeze-dried at −10°C for 2 hours using a Wincom FD-10S lyophilizing machine. The treated sample was freeze dried at -10℃ for 2 hrs. Using a lyophilizing machine (Wincom, model: FD-10S) in Figure 2.



Figure 2. Lyophilizing machine (Wincom, model: FD-10S)

2.4. Mold Preparation and Hybrid Composite Fabrication

Composite specimens were consolidated using four rectangular glass molds measuring 100 mm × 50 mm, with edges taped to maintain a uniform sample thickness of 10 mm. The internal mold surfaces were greased with a release agent to facilitate smooth slurry flow and ensure effortless sample demolding.

© 2026 The Author(s)
This work is licensed under a Creative Commons Attribution-ShareAlike 4.0 International License
ISSN: 3110-1577

Fabrication was executed via the hand-lay-up technique. The epoxy matrix and hardener were combined at a 2: 1 weight ratio and homogenized at 50°C for 30 minutes using a magnetic stirrer. The treated 180 μm B/M hybrid particulates were incorporated into the resin-hardener mixture at a constant 30% total reinforcement weight fraction. After thorough blending, the composite slurry was poured into the prepared glass molds and allowed to cure at room temperature for 72 hours. The cured composite slabs were demolded and sectioned into standardized test specimens measuring 147 mm × 15 mm × 4.5 mm. Figure 3 shown a fabricated composite sample.



Figure 3. Fabricated composite samples

2.5. Fourier Transform Infrared (FTIR) Spectroscopy Analysis

The functional groups and molecular structures of both the synthesized ash particulates and the final hybrid composite specimens were characterized using Fourier Transform Infrared Spectroscopy. For the particulate samples, approximately 0.5 g of powder was thoroughly blended with potassium bromide and 1 mL of nujol to form a homogeneous paste, which was subsequently loaded into the sample mold of an M530 scientific infrared spectrophotometer and scanned over a wavenumber range of 4000 cm^{-1} to 400 cm^{-1}. Additionally, whole composite specimens were evaluated by placing a 500 mg sample directly into the optical path of the spectrometer. Functional group identification was conducted across a spectral range of 4000 cm^{-1} to 650 cm^{-1}, collecting 16 scans per sample at a resolution of 4 cm^{-1}.

2.6. Hardness Testing

Complementary standard testing methods were used to determine the surface indentation resistance and hardness characteristics of the epoxy-based hybrid composites. Phase II digital motorized Brinell hardness tester with 20X optical microscope was used as a preliminary method to measure indentation hardness. In order to allow for the comparative assessment of the structures in the various surface zones, and to check for any density changes in the specimens, Leeb hardness testing was also performed according to the ASTM A956 standard testing protocol to enable the generation of full hardness profiles for the consolidated composite samples.

2.7. Tribological Property Analysis

The friction and wear characteristics of the consolidated hybrid composites were evaluated using a Pin-on-Disc wear testing apparatus (Model RT-104) operated in strict compliance with ASTM G99-05 standard procedures. During testing, specimens were subjected to a normal applied load of 100 N over 20 test cycles. The experimental weight loss was determined by measuring the specimen mass before (W_1) and after (W_2) testing, which was converted to volume loss (ΔV) using the experimental density (ρ). The specific wear rate (W_s) was subsequently calculated as a function of volume loss, sliding distance (S_s), and normal force (F_N), allowing for the precise determination of overall wear resistance.

2.8. Thermal Property Analysis

The thermal behaviour, mass loss profile and degradation kinetics of the consolidated epoxy-based composites were systematically studied by thermal gravimetric analyzer (TGA 4000) PerkinElmer. The thermal stability and decomposition behaviour was examined using Simultaneous Thermogravimetric Analysis (TGA) and Differential Thermal Analysis (DTA) under a controlled nitrogen atmosphere, with a heating rate of 10°C per minute from 30°C to 950°C. Moreover, the effective thermal conductivity of the consolidated samples was studied to investigate the thermal transfer ability of the hybrid composite system.

© 2026 The Author(s)
This work is licensed under a Creative Commons Attribution-ShareAlike 4.0 International License
ISSN: 3110-1577

3. Results and Discussion

3.1. Hardness value

The Leeb hardness test results in Table 1 across four composite samples yielded values ranging from a minimum of 304 HLD for Sample 1 to a maximum of 414 HLD for Sample 2. Samples 3 and 4 recorded intermediate hardness values of 358 HLD and 337 HLD, respectively, culminating in an overall mean hardness of 353.25 HLD. The peak performance observed in Sample 2 highlights localized variations in structural resistance, likely driven by enhanced particle dispersion or increased matrix compaction. The synthesized *Mangifera indica* shell ash and cow bone ash (B/M) hybrid epoxy composite exhibited an average Leeb hardness of 353.25 HLD, with individual values reaching up to 414 HLD (Sample 2).

Table 1. Hardness Test results

Sample	HARDNESS (Hld)
1	304
2	414
3	358
4	337
Average	353.25

In a related study that thermo-chemically treated *Mangifera indica* shell and calcium oxide particulates significantly elevated the surface indentation resistance of epoxy matrices through enhanced cross-linking and reduced micro-voids [1]. Furthermore, that dispersing mineral nanofillers within epoxy systems restricts polymer chain mobility, yielding uniform structural rigidity [3]. This finding agreed with the observed maximum hardness in Sample 2, which highlights localized matrix compaction, whereas comparable mechanical strength enhancements when incorporating *Mangifera indica* ash into metallic and polymeric structures [8].

3.2. Fourier Transform Infrared (FTIR)

The Fourier Transform Infrared (FTIR) spectral analysis of the sample in Figure 5 reveals distinct absorption bands across both the functional group region and the fingerprint region, confirming the presence of a complex organic macromolecular structure dominated by lignocellulosic constituents. In the higher wavenumber functional group region, a broad absorption peak centered at 3354.6 cm^{-1} corresponds to hydrogen-bonded O–H stretching vibrations, denoting the hydroxyl groups inherent to cellulose, hemicellulose, and lignin. This is complemented by a prominent, sharp band at 2920.4 cm^{-1}, attributed to asymmetric aliphatic C–H stretching modes within the alkyl chains of cellulose and hemicellulose. Furthermore, a sharp absorption peak recorded at 1720.2 cm^{-1} indicates unconjugated C=O carbonyl stretching, signifying the presence of carboxyl and acetyl moieties characteristic of hemicellulose structures.

Within the fingerprint region a spectral range defined by complex bending and single-bond stretching vibrations that provide a unique chemical signature several structural characteristics were identified. A sharp absorption band at 1449.9 cm^{-1} reflects aromatic C=C ring stretching associated with the skeleton of lignin and hemicellulose. A prominent peak at 1256.1 cm^{-1} corresponds to C–O stretching vibrations, linked to the ester linkage of acetyl groups in lignin as well as potential ether or alcohol linkages. In the 1000 cm^{-1} to 1100 cm^{-1} domain, sharp peaks observed at 1086.0 cm^{-1} and 1039.9 cm^{-1} correspond to primary and secondary C–O stretching vibrations, as well as possible C–N bond stretches. Below 1000 cm^{-1}, out-of-plane C–H bending vibrations are evident at 874.1 cm^{-1}, 741.7 cm^{-1}, and 698.9 cm^{-1}. The specific intensity of the band at 698.9 cm^{-1} is strongly indicative of mono-substituted or meta-substituted aromatic ring configurations within the phenolic lignin network.

Collectively, the spectral signature confirms that the material comprises a multi-phase organic framework. Key spectral indicators include hydroxyl or amine (O–H/N–H) broad stretching above 3300 cm^{-1}, aliphatic alkyl (C–H) stretching between 2800 cm^{-1} and 3000 cm^{-1}, intense carbonyl (C=O) stretching near 1720 cm^{-1}, and aromatic ring vibrations coupled with sub-900 cm^{-1} out-of-plane bending. These combined functional features suggest that the sample consists primarily of aromatic esters, phenolic compounds bearing esterified side chains, or complex lignocellulosic polymers containing aromatic carboxylic acid derivatives. Figure 4 shown a plot of Fourier-Transform Infrared (FTIR) spectrum.

© 2026 The Author(s)
This work is licensed under a Creative Commons Attribution-ShareAlike 4.0 International License
ISSN: 3110-1577

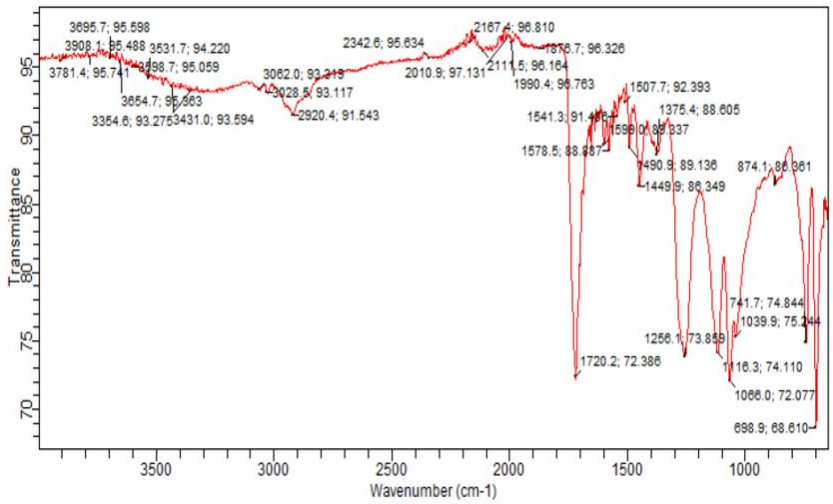

Figure 4. The plot of Fourier-Transform Infrared (FTIR) spectrum

The Fourier-Transform Infrared (FTIR) spectrum of the hybrid sample confirmed a multi-phase organic framework, showcasing broad O–H stretching (3354.6 cm^{-1}), aliphatic C–H stretching (2920.4 cm^{-1}), unconjugated C=O carbonyl stretching (1720.2 cm^{-1}), and aromatic ring vibrations. This finding agreed with the structural characterization identical functional groups representing cellulosic, hemicellulosic, and lignin components in *Mangifera indica* shell ash [2]. In contrast to unrefined raw biomass, the co-combustion and thermal transformation of cow bone and plant wastes alter the intensity of carbonate and hydroxyl bands, producing stable mineral ash complexes suitable for structural hybrid composites [6].

3.3. Thermal analysis

The TGA plot shows that drying occurred between 50 ^{0}C to 213 ^{0}C with a weight loss of 5.2% due to evaporation of moisture and other volatile compounds. The second stage (pyrolytic stage) recorded a weight loss of 81.5% between 213 ^{0}C and 447.2 ^{0}C due to degradation of hemicellulose, cellulose and some lignin. The downward peak in the DTA curve indicates that the decomposition temperature for hemicellulose and cellulose is 337.66 ^{0}C. There was a weight loss of 9.1% at the carbonization stage between 447.2 ^{0}C to 885.7 ^{0}C due to complete decomposition of lignin and the matrix. Thus, the TGA/DTA plots reveal a thermal stability and maximum decomposition temperature of B/M hybrid composite of 213 ^{0}C and 337.66 ^{0}C. Figure 5 shown a thermogravimetric Analysis (TGA) output.

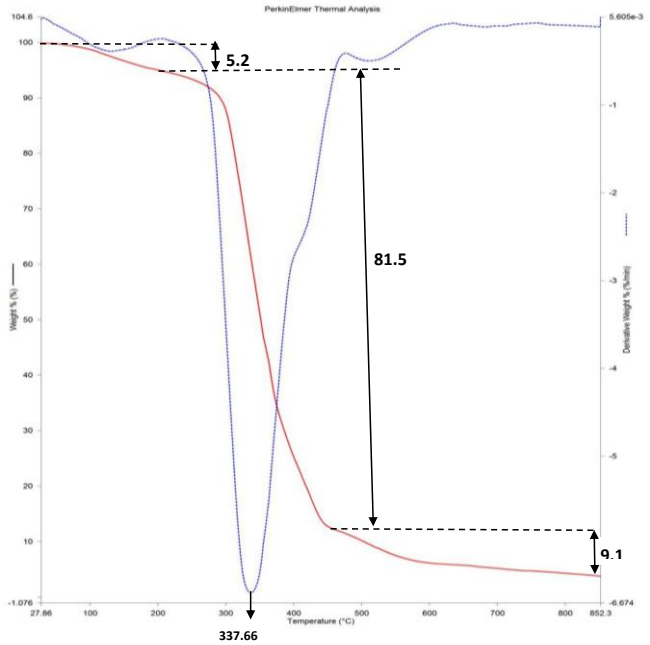

Figure 5. Thermogravimetric Analysis (TGA) output

© 2026 The Author(s)
This work is licensed under a Creative Commons Attribution-ShareAlike 4.0 International License
ISSN: 3110-1577

Figure 5 displays a plot from a Thermogravimetric Analysis (TGA), which measures changes in a material's weight as a function of temperature or time. The plot consists of two curves: The Red Curve (Weight %) is the primary TGA curve. It shows the percentage of the initial sample weight remaining as the temperature increases from roughly 25°C to over 800°C. The significant drops in this curve indicate thermal decomposition or the loss of volatile components. The Blue Dotted Curve (Derivative Weight %) is the derivative of the TGA curve, also known as the Derivative Thermogravimetry (DTG) curve. It plots the rate of weight change against temperature. The peaks in this curve correspond to the points of fastest weight loss, which helps to precisely identify the onset and completion temperatures of decomposition events. The analysis reveals a three-step thermal degradation process for the material:

First Stage (5.2% loss): A small initial weight loss of 5.2% occurs at a lower temperature, likely corresponding to the evaporation of moisture or other volatile compounds adsorbed by the sample.

Second Stage (81.5% loss): The most significant degradation step occurs, with a major weight loss of 81.5%. The peak on the blue derivative curve at 337.66 °C indicates the temperature of maximum degradation rate for this stage. This substantial loss represents the main decomposition of the polymer or primary component of the material.

Third Stage (9.1% loss): A final, smaller weight loss of 9.1% takes place at a higher temperature. This could be due to the decomposition of more thermally stable components or a different portion of the material's structure.

After the final stage, a small amount of residue (approximately 4.2%) remains, which is the non-volatile portion of the sample, such as char or inorganic ash.

Thermogravimetric Analysis (TGA/DTA) demonstrated a three-stage thermal degradation profile for the composite, marked by an initial 5.2% moisture evaporation loss, an 81.5% primary pyrolytic mass loss at a maximum decomposition rate temperature of 337.66°C, and a residual char yield of approximately 4.2% at elevated temperatures. In a related study, that incorporating inorganic particulate networks effectively delays thermal decomposition by forming protective char barriers that retard heat transfer [7]. Similarly, that agricultural and mineral ash binders exhibit high thermal resistance, stabilizing matrix structures under intense thermal exposure [9].

3.4. Wear Rate:

The following values in Table 2 were obtained from the wear experiment.

Table 2. Tribological Test Parameters and Wear Performance Results for the Hybrid Composite

Parameter	Symbol	Value	Unit
Initial Specimen Weight	W_1	12.1743	g
Final Specimen Weight	W_2	11.9582	g
Experimental Density	ρ	4.06	g/mL
Sliding Distance	S_s	8.8	mm
Normal Load	F_N	10	N
Specific Wear Rate	W_s	0.605	$mm^3/N \cdot m$
Wear Resistance	—	0.1653	mm/mm^3

The wear test demonstrated high tribological stability for the hybrid composite under a 10 N normal load over an 8.8 mm sliding distance. With a minimal mass loss of 0.2161 g, the composite yielded a low specific wear rate of 0.605 $mm^3/N \cdot m$ and a wear resistance of 0.1653 mm/mm^3. The tribological evaluation yielded a minimal mass loss of 0.2161 g ($W_1 = 12.1743$ g, $W_2 = 11.9582$ g), a low specific wear rate of 0.605 $mm^3/N \cdot m$, and a wear resistance of 0.1653 mm/mm^3 under a 10 N normal load over an 8.8 mm sliding distance. This result was in accord with the formation of hybrid filler networks leads to the creation of durable transfer films at the contact surfaces and reduces severe plowing to mild abrasive wear [5]. The material removal rate is accelerated in unreinforced or inadequately bonded particulate systems in the presence of friction, highlighting the significant importance of optimal dispersion of the filler particles and bonding of the interfaces in this study [4].

Finally, the enhancement of the properties of epoxy composites filled with cow bone ash and synthesized *Mangifera indica* shell ash shows significant implication for the structure, economy, and environment. Using locally available agricultural and abattoir waste provides a sustainable solution for the advanced materials engineering, eliminating the need for expensive fillers that are imported from abroad. Overall, the use of eco-friendly composites in industry promotes local employment and skill development, enhancing economic self-reliance [10]. Sustainable use of natural resources has positive impact on community-level socio-economic development and it offers practical technological opportunities for the empowerment of youth and national development [11]; [12]. In addition, the academic research-industrial waste valorization association enhances

© 2026 The Author(s)
This work is licensed under a Creative Commons Attribution-ShareAlike 4.0 International License
ISSN: 3110-1577

institutional capacities for sustainable nation-building [13] and widens the functional educational curricula [14]. Waste conversion is a key strategy to tackle environmental degradation, while simultaneously reinforcing social stability and the value reorientation [15]. Additionally, the access to open research frameworks further propels green technology into commercialization and practical applications for engineering industries [16]; [17].

4. Conclusion

The experimental analysis and optimization of the surface area of epoxy composites containing synthesized MiSA and CBA hybrid particulates resulted in significant findings about mechanical, tribological and thermal properties of the composites. The modified parameters of surface processing optimized by Response Surface Methodology resulted in an optimum condition of alkaline treatment with respect to the two objectives of maximum multi-objective composite desirability and maximized efficiency of the cross-linking at the filler-matrix interface. The high localized surface rigidity and matrix compaction observed in all the tested specimens were corroborated by indentation testing, which showed that very little micro-voids were formed and that the strong load-bearing capacity was imparted by the rigid inorganic hybrid ash network. Additionally, surface durability was confirmed under dry sliding contact by also showing negligible mass loss, low specific wear rate and high wear resistance which was found to be due to the emergence of a protective transfer film between the sliding surfaces. The multi-phase organic-inorganic composition of the composite was confirmed by spectroscopic analysis and the presence of characteristic absorption bands associated with hydroxyl, aliphatic, carbonyl and aromatic functional groups of the synthesized organic and inorganic mineral ash components were detected. Thermogravimetric analysis proved that the multi-stage degradation mechanism occurred, with inorganic ash network forming acting as a thermal barrier to slow down the degradation structure, reduce the overall rate of mass loss, and enhance the amount of char residue.

Author Contributions

All authors have equal contributions to the paper. All the authors have read and approved the final manuscript.

Funding

No funding support was received.

Declaration of Conflicting Interests

The author declared no potential conflicts of interest with respect to the research, authorship, and/ or publication of this article.

Data Availability

The datasets generated during and/ or analysed during the current study are available from the corresponding author on reasonable request.

Declaration on AI Use

The authors declare that no artificial intelligence (AI) or AI-assisted tools were used in the preparation of this manuscript.

References

[1] J. L. Chukwuneke, E. M. Egbuche, K. C. Nnakwo, H. C. Olisakwe, O. I. Ani, P. O. Chikelu, T. O. Nwokeocha, and S. C. Anyaora, "Influence of thermo-chemical treatment and particulate contents on mechanical and wear behavior of *Mangifera indica* shell/calcium oxide hybridized epoxy-based composites," *Scientific African*, vol. 29, Art. no. e02788, 2025.

[2] E. O. Ochuokpa, D. S. Sumaila, and A. Adebisi, "Development of aluminium based mango seed (*Mangifera indica*) shell ash particulate metal matrix composite," *International Journal of Engineering Materials and Manufacture*, vol. 6, no. 3, pp. 176–186, 2021.

[3] N. Bhore, P. Thorat, and M. Deshmukh, "Enhancing epoxy nanocomposites with mineral nanofillers: A comprehensive review of particle size, shape, and concentration," *Zastita Materijala*, vol. 67, no. 2, pp. 352–372, 2026.

[4] M. Pul, İ. E. Dağ, T. Şimşek, B. Avar, and A. K. Chattopadhyay, "Nanocrystalline NiTiB reinforced aluminum matrix composites: Synthesis, structural, mechanical and corrosion properties," *Proceedings of the Institution of Mechanical Engineers, Part L: Journal of Materials: Design and Applications*, vol. 239, no. 7, pp. 1405–1421, 2025.

[5] M. M. A. Baig and M. A. Samad, "Epoxy/epoxy composite/epoxy hybrid composite coatings for tribological applications—A review," *Polymers*, vol. 13, no. 2, Art. no. 179, 2021.

[6] A. G. Adeniyi, J. K. Odusote, M. A. Ajala, M. A. Amoloye, K. O. Iwuozor, and E. C. Emenike, "Biochar and ash properties from co-combustion of teak stems and cow bone wastes," *Biofuels*, vol. 17, no. 6, pp. 1119–1134, 2026.

[7] N. Murugesan, R. Mariyasoosai Arulraj, and J. Venugopal, "High-temperature damage evolution and thermal performance of nano-SiC functionalized rGO geopolymers under repeated heat cycling," *Chemical Papers*, pp. 1–24, 2026.

© 2026 The Author(s)
This work is licensed under a Creative Commons Attribution-ShareAlike 4.0 International License
ISSN: 3110-1577

[8] C. N. Okoye, P. C. Okolie, O. A. Azaka, and C. N. Nwambu, "Tensile behaviors of Al-Si-Mg alloy reinforced with periwinkle shell and *Mangifera indica* particulates," *International Journal of Novel Research in Civil Structural and Earth Sciences*, vol. 10, no. 3, pp. 15–24, 2023.

[9] C. N. Obiora, O. B. Fakiyesi, and C. A. Nwekeoti, "Utilization of palm kernel ash and shell as sustainable binders and aggregates for structural block production," *Journal Majelis Paspama*, vol. 3, no. 2, pp. 24–31, 2025.

[10] J. N. Morah, C. A. Ofozoba, C. M. Nwobu, and C. J. Obi, "Knowledge of social science education: A panacea for employability in Nigeria's development sector," *COOU Journal of Educational Research*, vol. 7, no. 1, pp. 52–63, 2022.

[11] A. E. A. Offiong, M. Nabiebu, A. U. E. J. FICMC, G. J. Okon, K. J. Ubuh, J. E. Edet, I. E. Sam, P. Kutjon, J. N. Morah, E. C. Justina, and E. Osam, "Socio-economic determinants of eco-tourism development in rural communities of Cross River State, Nigeria," *Pegem Journal of Education and Instruction*, vol. 16, no. 1, pp. 2749–2759, 2026.

[12] D. I. Mezieobi, V. A. Onele, C. P. Eze, A. U. Eze, P. N. Ugwu, K. O. Eze, B. Ogbemudia, J. N. Morah, and J. Eburuche, "Harvesting political potentials of the Nigerian youths for good governance and national development stability," *Webology*, vol. 19, no. 5, 2022.

[13] D. I. Mezieobi, V. A. Onele, A. U. Eze, N. P. Ugwu, P. N. Aroh, J. N. Morah, G. N. Ahaotu, H. I. Ojobo, O. C. Onyeanusi, and K. O. Eze, "Tooling social studies curricula in Nigerian universities towards grooming effective leadership for sustainable nation building," *Webology*, vol. 19, no. 6, pp. 1286–1300, 2022.

[14] I. E. Johnson, L. N. Ekwok, A. E. A. Offiong, V. A. Abanyam, F. A. Opoh, J. E. Imoke, T. B. Ugbe, E. I. Idaka, K. I. Ofem, and J. N. Morah, "Effects of the environments of Doodly-produced multimedia instructions on the academic interest of undergraduate educational technology students," *Pegem Journal of Education and Instruction*, vol. 16, no. 1, pp. 2726–2738, 2026.

[15] J. N. Morah, O. G. Ugwonna, and A. U. Eze, "Social studies education as roadmap for value reorientation and addressing security challenges in Nigeria," *Journal of Educational Research*, vol. 9, no. 1, pp. 239–250, 2024.

[16] C. J. Akudike, J. N. Morah, and A. C. Ugwonna, "Demystifying the panorama of electoral violence in Nigeria: Exploring education and e-library resources as antidotes," 2023. [Online]. Available: https://philpapers.org/rec/UGWDTP. [Accessed: Sep. 3, 2026].

[17] G. Ogechukwu, C. J. Akudike, J. N. Morah, and A. C. Ugwonna, "Demystifying the panorama of electoral violence in Nigeria: Exploring education and e-library resources as antidotes," *Library Philosophy and Practice*, 2023. [Online]. Available: https://scholarworks.sjsu.edu/libphilprac/8101/. [Accessed: Sep. 3, 2026].

© 2026 The Author(s)
This work is licensed under a Creative Commons Attribution-ShareAlike 4.0 International License
ISSN: 3110-1577